European Journal of Mechanics A/Solids 31 (2011) 13–20

Contents lists available at ScienceDirect

European Journal of Mechanics A/Solids

journal homepage: www.elsevier.com/locate/ejmsol

Exact solutions for nonlinear static responses of a shear deformable FGM beam under an in-plane thermal loading

L.S. Ma [a,b,*], D.W. Lee [b]

[a] School of Science, Lanzhou University of Technology, Lanzhou 730050, China
[b] MEMS & Nanotechnology Laboratory, School of Mechanical Systems Engineering, Chonnam National University, Gwangju 500-757, Republic of Korea

ARTICLE INFO

Article history:
Received 13 August 2010
Accepted 19 June 2011
Available online 19 July 2011

Keywords:
Functionally graded material beam
Exact solution
Static response
In-plane thermal loading
Transverse shear deformation

ABSTRACT

An exact, closed-form solution is obtained for the nonlinear static responses of beams made of functionally graded materials (FGM) subjected to a uniform in-plane thermal loading. The equations governing the axial and transverse deformations of FGM beams are derived based on the nonlinear first-order shear deformation beam theory and the physical neutral surface concept. The three equations are reduced to a single nonlinear fourth-order integral–differential equation governing the transverse deformations. For a fixed–fixed FGM beam, the equation and the corresponding boundary conditions lead to a differential eigenvalue problem, while for a hinged–hinged FGM beam, an eigenvalue problem does not arise due to the inhomogeneous boundary conditions, which result in quite different behavior between clamped and simply supported FGM beams. The nonlinear equation is directly solved without any use of approximation and a closed-form solution for thermal post-buckling or bending deformation is obtained as a function of the applied thermal load. The exact solutions explicitly describe the nonlinear equilibrium paths of the deformed beam and thus are able to provide insight into deformation problems. To show the influence of the material gradients, transverse shear deformation, in-plane loading, and boundary conditions, numerical examples are given based on exact solutions, and some properties of the post-buckling and bending responses of FGM beams are discussed. The exact solutions obtained herein can serve as benchmarks to verify and improve various approximate theories and numerical methods.
© 2011 Elsevier Masson SAS. All rights reserved.

1. Introduction

It is difficult to obtain an exact solution of the nonlinear equations in large deflection problems of a beam-like structure due to the intractability of the geometric nonlinear control equations of large deflection beams. Thus far, only a few exact solutions have been investigated. However, with progress in science and technology, a need arises in engineering practice to accurately predict the nonlinear static responses of large deflection beams.

Functionally graded materials (FGM) structures are those in which the volume fractions of two or more materials are varied continuously as a function of position along certain dimension(s) of the structure to achieve a required function. Typically, FGMs are made from a mixture of ceramic and metal. This paper is concerned with obtaining exact solutions for the nonlinear static responses of beams made of a metal/ceramic functionally graded materials under an in-plane thermal loading. Based on the exact solutions, an investigation was conducted on the post-buckling or bending behavior of FGM beams. The present investigation indicates that a hinged–hinged FGM beam subjected to an in-plane thermal load does exhibit some characteristics that are quite different from those of a fixed–fixed FGM beam.

Many studies have been conducted on the static behavior of FGM beams. Librescu et al. (2005) studied the behavior of thin-walled beams made of FGMs that operated at high temperatures, which included vibration and instability analysis with the effects of the volume fraction, temperature gradients, etc. A review of various investigations on FGM including thermo-mechanical studies is found in Birman and Byrd (2007). Employing the finite element method, Bhangale and Ganesan (2006) investigated the thermoelastic buckling and vibration behavior of an FGM sandwich beam. Based on the two-dimensional theory of elasticity and using the state-space method, Ying et al. (2008) presented solutions for the bending and free vibration of FG beams resting on a Winkler–Pasternak elastic foundation. Static, free, and wave propagation analyses were carried out by Chakraborty et al. (2003) to

* Corresponding author. MEMS & Nanotechnology Laboratory, School of Mechanical Systems Engineering, Chonnam National University, Gwangju 500-757, Republic of Korea. Tel./fax: +86 62 530 1684.
E-mail address: mems@chonnam.ac.kr (L.S. Ma).

0997-7538/$ – see front matter © 2011 Elsevier Masson SAS. All rights reserved.
doi:10.1016/j.euromechsol.2011.06.016

examine behavioral differences in FGM beams. Using an efficient, third-order zigzag theory for estimating the effective modulus of elasticity, Kapuria et al. (2008) presented a finite element model for the static and free-vibration responses of layered FGM beams along with an experimental validation for two different FGM systems under various boundary conditions. Yang and Chen (2008) studied the free vibration and elastic buckling of FGM beams with open edge cracks by using classical beam theory. Li (2008) proposed a new unified approach to investigate the static and free vibration behavior of Euler–Bernoulli and Timoshenko beams. Zhong and Yu (2007) presented a general two-dimensional solution for a cantilever beam in terms of the Airy stress function.

As the aforementioned works show, research on the exact solution for the nonlinear static responses of FGM beams subjected to a thermal load is scarce and the present work attempts to fill this gap. Emama and Nayfeh (2009) obtained a closed-form solution for the post-buckling configurations of composite beams with various boundary conditions based on the classical beam theory and expressed these configurations as functions of the applied axial load. In this study, we extend their work to a shear deformable FGM beam.

In static analysis, the variation in material properties along the thickness of FGM plates or beams results in quite a different behavior compared to that of plates or beams made of pure materials. For example, bifurcation buckling generally cannot occur for FGM plates or beams with simply supported edges due to in-plane loadings, that is, a transverse deflection is initiated, regardless of the magnitude of the loading, as is often the case with laminated composite materials (Leissa, 1986; Leissa, 1987; Qatu and Leissa, 1993). The phenomenon was taken note of by Shen (2004) and Aydogdu (2008). Shen (2004) stated that bifurcation buckling does not take place for FGM rectangular plates with simply supported edges due to the bending-stretching coupling. In the past, several analyses have been published regarding the buckling of FGM plates where such buckling cannot physically exist, as pointed out by Qatu and Leissa (1993). The flatness conditions of an FGM plate during the pre-buckling stage were presented by Aydogdu (2008). However, a few investigators have further examined these special behavior of FGM plates or beams in detail. Shen (2002) analyzed the influence of various factors such as the thermal loading and in-plane boundary conditions on the nonlinear bending of FGM plates. The nonlinear bending and post-buckling of an FGM circular plate under a thermal loading and uniform radial pressure, respectively, was investigated by Ma and Wang (2003a, b). They found that transverse deflections occur immediately when an in-plane compressive load is applied to a simply supported FGM circular plate.

To the authors' knowledge, only a few researchers have given considerable attention to the static behavior of FGM beams with simply supported edges due to an in-plane loading, which is one of the primary objectives of the present investigation.

The stretching–bending coupling in the constitutive equations of an FGM plate does not exist when the coordinate system is located at the physical neutral surface of the plate (Morimoto et al., 2006; Zhang and Zhou, 2008). Therefore, the governing equations and boundary conditions for the FGM plate can be simplified. In the present investigation, based on the nonlinear classical beam theory and the physical neutral surface concept, the governing equations for the static behavior of FGM beams subjected to a uniform in-plane thermal loading are derived. The two equations can be reduced to a single nonlinear fourth-order integral–differential equation that governs the transverse deformations. For a fixed–fixed FGM beam, the equation and the corresponding boundary conditions lead to a differential eigenvalue problem, but for a hinged–hinged FGM beam, an eigenvalue problem does not arise due to the inhomogeneous boundary conditions, which result in quite different behavior between clamped and simply supported FGM beams. The nonlinear equation is directly solved without any use of approximation and a closed-form solution for the thermal post-buckling or bending deformation is obtained as a function of the applied thermal load. The exact solutions explicitly describe the nonlinear equilibrium paths of the deformed beam and thus, are able to provide insights into deformation problems. Also, the exact solution for simply supported beams indicates that the number of possible solution branches for the beams is infinite. To show the influence of the material gradients, transverse shear deformation, in-plane loading, and boundary conditions, numerical examples based on the exact solutions are given, and some properties of the post-buckling and bending responses of FGM beams are discussed. The exact solutions obtained herein are in good agreement with those obtained by numerical methods.

2. Basic equations

A beam made of functionally graded materials with a uniform cross-section of area A, height h, and length l is considered here. The Cartesian coordinate system, (x, y, z), with the origin at the left end of the beam is used in this analysis. The xoy plane is taken to be the undeformed mid-plane of the beam, the x axis coincides with the centroidal axis of the beam, and the z axis is perpendicular to the x–y plane, its positive direction being toward the height of the cross-section.

It is assumed that the material properties of the form, P (such as the Young's modulus, E, and the thermal expansion coefficient, α), of the beam vary along the height of the beam, and can be expressed as follows (Ma and Wang, 2003a).

$$P(z) = (P_m - P_c)\left(\frac{h-2z}{2h}\right)^n + P_c. \tag{1}$$

Here, the subscripts, m and c, denote the metallic and ceramic constituents, respectively, and n is the gradient index. In this paper, Poisson's ratio, ν, is assumed to be a constant.

Based on the physical neutral surface concept put forward by Zhang and Zhou (2008), the physical neutral surface of an FGM beam is given by $z = z_0$.

$$z_0 = \frac{\int_{-h/2}^{h/2} zE(z)\mathrm{d}z}{\int_{-h/2}^{h/2} E(z)\mathrm{d}z}. \tag{2}$$

It can be seen that the physical neutral surface and the geometric middle surface are the same in a homogeneous isotropic beam.

Using the physical neutral surface concept and the first-order shear deformation beam theory (FBT), the displacements take the following form.

$$\begin{aligned} U_x(x,z) &= u(x) + (z-z_0)\phi(x) \\ U_z(x,z) &= w(x). \end{aligned} \tag{3}$$

Here, u and w are the displacements in the physical neutral surface along the coordinates, x and z, respectively. φ denotes the slope at $z = z_0$ of the deformed line that was straight in the undeformed beam. The strains are as follows.

$$\begin{aligned} \varepsilon_x &= \varepsilon_x^0 + (z-z_0)\varepsilon_x^1 = \left\{\frac{\mathrm{d}u}{\mathrm{d}x} + \frac{1}{2}\left(\frac{\mathrm{d}w}{\mathrm{d}x}\right)^2\right\} + (z-z_0)\frac{\mathrm{d}\phi}{\mathrm{d}x} \\ \gamma_{xz} &= \gamma_{xz}^0 = \phi + \frac{\mathrm{d}w}{\mathrm{d}x}. \end{aligned} \tag{4}$$

In the above, ε_x^0 and ε_x^1 are the strain and curvature in the physical neutral surface, respectively. The constitutive equations can be deduced by proper integration.

$$N_x = A_x\left\{\frac{du}{dx}+\frac{1}{2}\left(\frac{dw}{dx}\right)^2\right\} - N^T. \tag{5a}$$

$$M_x = D_x\frac{d\phi}{dx} - M^T. \tag{5b}$$

$$Q_x = A_{xz}\left(\phi+\frac{dw}{dx}\right). \tag{5c}$$

Here, $A_x = \int_A E(z)dA$, $A_{xz} = k_s\int_A E(z)/2(1+\nu)dA$, $D_x = \int_A (z-z_0)^2 E(z)dA$, $(N^T, M^T) = \int_A E\alpha\Delta T\{1,(z-z_0)\}dA$, k_s denotes the shear correction factor and ΔT is the uniform temperature rise.

It can be seen that there is no stretching-bending coupling in the constitutive equations of the physical neutral surface theory.

Using the energy principle, one can derive the following equilibrium equations and boundary conditions based on FBT.

$$\frac{d}{dx}\left\{A_x\left\{\frac{du}{dx}+\frac{1}{2}\left(\frac{dw}{dx}\right)^2\right\} - N^T\right\} = 0. \tag{6}$$

$$D_x\frac{d^2\phi}{dx^2} - A_{xz}\left(\phi+\frac{dw}{dx}\right) = 0. \tag{7}$$

$$A_{xz}\left(\frac{d\phi}{dx}+\frac{d^2w}{dx^2}\right) + \left[A_x\left\{\frac{du}{dx}+\frac{1}{2}\left(\frac{dw}{dx}\right)^2\right\} - N^T\right]\frac{d^2w}{dx^2} = 0. \tag{8}$$

$$u = 0,\ w = 0,\ \phi = 0 \quad \text{for a fixed end.} \tag{9a}$$

$$u = 0,\ w = 0,\ D_x\frac{d\phi}{dx} - M^T = 0 \quad \text{for a hinged end.} \tag{9b}$$

3. Solution

Integrating Eq. (6), one obtains:

$$A_x\left\{\frac{du}{dx}+\frac{1}{2}\left(\frac{dw}{dx}\right)^2\right\} - N^T = A_1. \tag{10}$$

The substitution of Eq. (10) into Eq. (8) leads to:

$$A_{xz}\left(\frac{d\phi}{dx}+\frac{d^2w}{dx^2}\right) + A_1\frac{d^2w}{dx^2} = 0. \tag{11}$$

Differentiating Eq. (7) with respect to x, one obtains:

$$A_{xz}\left(\frac{d\phi}{dx}+\frac{d^2w}{dx^2}\right) = D_x\frac{d^3\phi}{dx^3}. \tag{12}$$

The substitution of Eq. (12) into Eq. (11) leads to:

$$D_x\frac{d^3\phi}{dx^3} + A_1\frac{d^2w}{dx^2} = 0. \tag{13}$$

Calculating the second-order derivative of Eq. (11), one obtains:

$$\frac{d^3\phi}{dx^3} = -\left(1+\frac{A_1}{A_{xz}}\right)\frac{d^4w}{dx^4}. \tag{14}$$

Substituting Eq. (14) into Eq. (13), we obtain:

$$D_x\left(1+\frac{A_1}{A_{xz}}\right)\frac{d^4w}{dx^4} - A_1\frac{d^2w}{dx^2} = 0. \tag{15}$$

Eq. (10) can be rewritten as:

$$\frac{du}{dx} = -\frac{1}{2}\left(\frac{dw}{dx}\right)^2 + \frac{N^T}{A_x} + \frac{A_1}{A_x}. \tag{16}$$

The integration of Eq. (16) yields:

$$u = -\frac{1}{2}\int_0^x\left(\frac{dw}{d\eta}\right)^2 d\eta + \frac{N^T}{A_x}x + \frac{A_1}{A_x}x + A_2. \tag{17}$$

Through the application of the boundary conditions given by Eq. (9a) and (9b), Eq. (17) leads to:

$$A_1 = \frac{A_x}{2l}\int_0^l\left(\frac{dw}{dx}\right)^2 dx - N^T. \tag{18}$$

$$A_2 = 0. \tag{19}$$

Substituting Eq. (18) into Eq. (15), we obtain:

$$D_x\left\{1 - \frac{1}{A_{xz}}\left[N^T - \frac{A_x}{2l}\int_0^l\left(\frac{dw}{dx}\right)^2 dx\right]\right\}\frac{d^4w}{dx^4} + \left[N^T - \frac{A_x}{2l}\int_0^l\left(\frac{dw}{dx}\right)^2 dx\right]\frac{d^2w}{dx^2} = 0. \tag{20}$$

Eq. (20) governs the transverse response of a geometrically nonlinear FGM beam. Eq. (11) can be rewritten as follows

$$A_{xz}\frac{d\phi}{dx} + (A_{xz}+A_1)\frac{d^2w}{dx^2} = 0. \tag{21}$$

Integrating Eq. (21) yields

$$A_{xz}\phi = -(A_{xz}+A_1)\frac{dw}{dx} + B_1. \tag{22}$$

Through the application of the symmetric conditions given by $\phi(l/2) = 0$ and $dw/dx(l/2) = 0$ leads to $B_1 = 0$ in Eq. (22). So, the boundary condition, $\phi = 0$, for a fixed end can be converted into $dw/dx = 0$, while $D_x(d\phi/dx) - M^T = 0$ for a hinged end can be converted into $d^2w/dx^2 + A_{xz}/D_x(A_{xz}+A_1)M^T = 0$.

For generalizing the subsequent results, we use the following non-dimensional variables:

$$X = \frac{x}{l};\quad W = \frac{w}{r};\quad N = \frac{N^T l^2}{D_x};\quad M = \frac{M^T l^2}{D_x r};\quad \beta = \frac{A_x r^2}{D_x};\quad F_1 = \frac{D_x}{A_{xz} l^2} \quad \text{and} \quad \lambda = 12\left(\frac{l}{h}\right)^2\alpha_m\Delta T,$$

where $r = \sqrt{I/A}$ is the radius of gyration of the cross-section. As a result, we write Eq. (20) as follows:

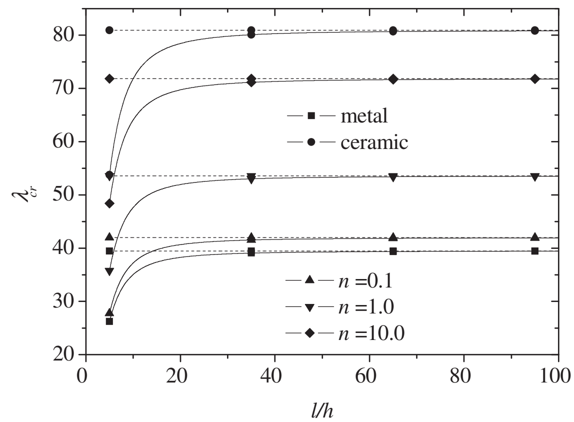

Fig. 1. Variation of the dimensionless critical thermal buckling load, λ_{cr}^F, of a fixed–fixed FGM beam with the slenderness ratio, l/h.

$$\frac{d^4W}{dX^4}+a^2\frac{d^2W}{dX^2} = 0. \tag{23}$$

Here, a^2 represents an eigenvalue of Eq. (23) that is defined by:

$$a^2 = \frac{k^2}{1-F_1k^2}. \tag{24}$$

and

$$k^2 = N-\frac{\beta}{2}\int_0^1\left(\frac{dW}{dX}\right)^2 dX. \tag{25}$$

The boundary conditions are given by the following.

$$W = 0 \quad \text{and} \quad \frac{dW}{dX} = 0 \quad \text{for a fixed end}\,. \tag{26}$$

$$W=0 \;\; \text{and} \;\; \frac{d^2W}{dX^2}+\left(1+F_1a^2\right)M=0 \;\; \text{for a hinged end}\,. \tag{27}$$

We should note that for a fixed–fixed FGM beam, Eq. (23) and the corresponding boundary conditions, viz., Eq. (26), lead to a differential eigenvalue problem, but for a hinged–hinged FGM beam, an eigenvalue problem does not arise due to the inhomogeneous boundary conditions. The discrepancy between the two beams results in quite different behavior between an FGM beam with clamped boundary conditions and one with simply supported boundary conditions, as will be presented in Sections 3.1 and 3.2.

When the transverse shear stiffness $A_{xz} \to \infty$, Eq. (23) and the boundary conditions, Eqs. (26) and (27), can reduce to those based on the classical beam theory, which indicates that the effect of transverse shear deformation is ignored.

3.1. *Postbuckling of a fixed–fixed FGM beam*

The solution of Eq. (23) can be written as follows:

$$W(X) = C_1\sin(aX)+C_2\cos(aX)+C_3X+C_4. \tag{28}$$

whereC_1, C_2, C_3 and C_4 are constants of integration.

For a fixed–fixed beam, its boundary conditions, viz., Eq. (26), can be used to give the following equations:

$$W(0) = C_2+C_4 = 0. \tag{29a}$$

$$W(1) = C_1\sin a+C_2\cos a+C_3+C_4 = 0. \tag{29b}$$

$$W'(0) = C_1a+C_3 = 0. \tag{29c}$$

$$W'(1) = C_1a\cos a-C_2a\sin a+C_3 = 0. \tag{29d}$$

Using Eqs.(29a), (29b) and (29c), we arrive at

$$C_1 = \frac{\cos a-1}{\sin a-a}c,\;\; C_2 = -c,\;\; C_3 = -a\frac{\cos a-1}{\sin a-a}c,\;\; C_4 = c\,. \tag{30}$$

Thus, a closed-form solution for the buckled configuration of beams with fixed–fixed boundary conditions is given by:

$$W(X)=c\left\{\frac{\cos a-1}{\sin a-a}\sin(aX)-\cos(aX)-\frac{a(\cos a-1)}{\sin a-a}X+1\right\}. \tag{31}$$

Here, c is a constant related to the applied thermal load, N, and is given by:

$$c = \pm\frac{2}{\sqrt{\beta\left(1+F_1a^2\right)}}\sqrt{\frac{N}{a^2}\left(1+F_1a^2\right)-1}. \tag{32}$$

Substituting the expressions in Eq. (30) into Eq. (29d), we obtain:

$$2-2\cos a-a\sin a = 0. \tag{33}$$

Eq. (33) is the characteristic equation for a of a beam with fixed–fixed boundary conditions.

From Eq. (33), one can easily obtain the eigenvalues; the lowest eigenvalue is $a_1 = 2\pi$. At the beginning stage of buckling, the configuration of a buckled beam is sufficiently close to the beam's initial straight configuration. In this case, the thermal load, N, at that instant of time is the critical buckling thermal load,N_{cr}^F. One can obtain the critical buckling load, N_{cr}^F, from Eq. (32) by letting $c=0$, that is, $N_{cr}^F = a_1^2/1+F_1a_1^2$. Thus, the analytical relation between the dimensionless critical buckling thermal load, λ_{cr}^F, of a fixed–fixed FGM beam and the gradient index, n, is given by:

$$\lambda_{cr}^F = a_1^2\frac{C_n}{1+F_1a_1^2}. \tag{34}$$

where C_n is a constant related to the gradient index, n. Eq. (34) becomes the classical dimensionless critical buckling thermal load, λ_{cr}^C, by letting $F_1 = 0$ (i.e., the transverse shear stiffness $A_{xz}\to\infty$), which gives,$\lambda_{cr}^C = a_1^2C_n$. Thus, Eq. (34) also represents the analytical relationship between the dimensionless critical buckling thermal loads based on FBT and CBT, that is,

$$\lambda_{cr}^F = \lambda_{cr}^C\frac{1}{1+F_1a_1^2}. \tag{35}$$

Letting $n=0$, the FGM beam becomes homogeneous one. For the first-order buckling mode, $a = 2\pi$, using Eqs.(31), (32) and (35), one can easily obtain the solution provided by the Timoshenko beam theory for a fixed–fixed homogeneous beam:

Table 1
Material properties of Si_3N_4 and SUS304.

Materials	Properties ($T = 300$ K)	
	E [Pa]	α [1/K]
Si_3N_4	322.27e+9	7.4746e-6
SUS304	207.79e+9	15.3210e-6

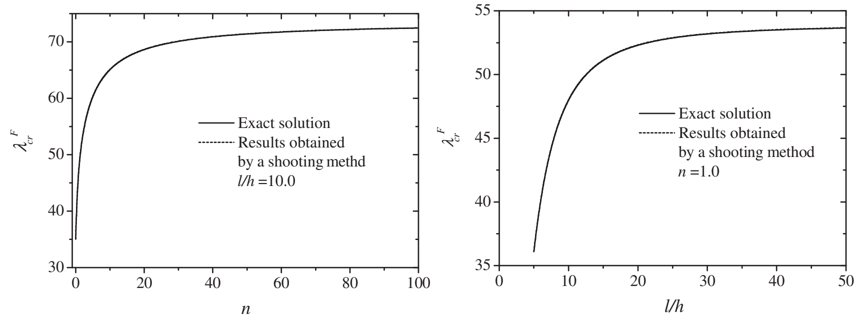

Fig. 2. Comparison of the present exact solution for the critical thermal buckling load of a fixed–fixed FGM beam with numerical results obtained by a shooting method.

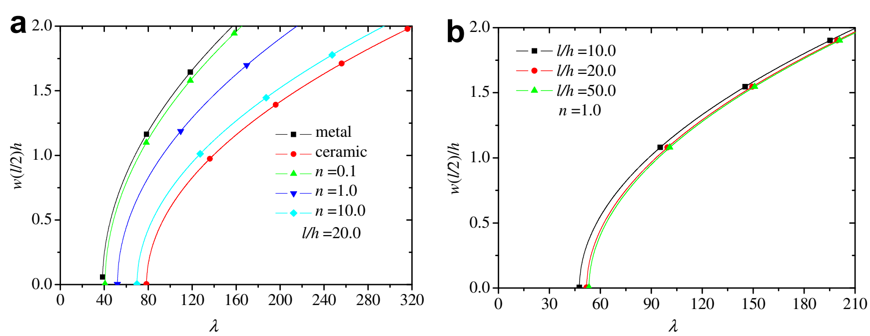

Fig. 3. Post-buckling paths of FGM beams clamped at both ends.

$$W(X) = c[1 - \cos(2\pi X)]. \tag{36}$$

where

$$c = \frac{2}{\sqrt{1+4\pi^2F_1}}\sqrt{\frac{\lambda}{4\pi^2}\left(1+4\pi^2F_1\right) - 1},$$

and

$$\lambda_{cr}^F = \frac{4\pi^2}{1+4\pi^2F_1}. \tag{37}$$

Eq. (37) is identical to the solution obtained by Ma et al. (2006).

Fig. 1 demonstrates the variation of the dimensionless critical thermal buckling load, λ_{cr}^F, with the slenderness ratio, l/h, based on FBT for various values of the gradient index, n. Also shown in Fig. 1 through dashed lines are the classical results. The material properties used in Fig. 1 are given in Table 1. It is seen from Fig. 1 that as the slenderness ratio, l/h, increases, the critical buckling temperature increases up to the classical results. Such a trend is observed because the effect of the transverse shear deformation is ignored in the classical beam theory.

Now, we analyze the load-deflection response of a fixed–fixed FGM beam based on the exact solution. The midspan deflection of the beam, which corresponds to the lowest eigenvalue, is given by:

$$W\left(\frac{1}{2}\right) = \pm\frac{4}{\sqrt{\beta\left(1+F_1a^2\right)}}\sqrt{\frac{N}{a^2}\left(1+F_1a^2\right) - 1}. \tag{38}$$

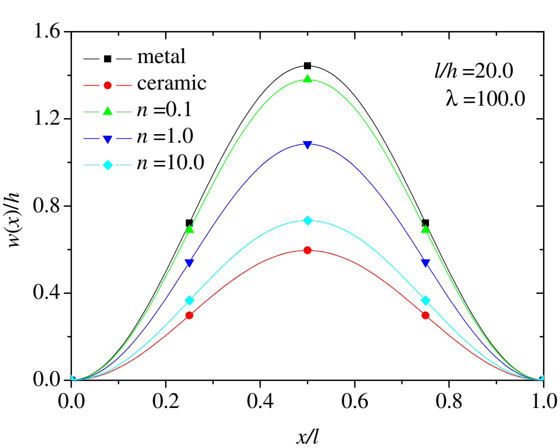

Fig. 4. Postbuckling configurations of FGM beams clamped at both ends.

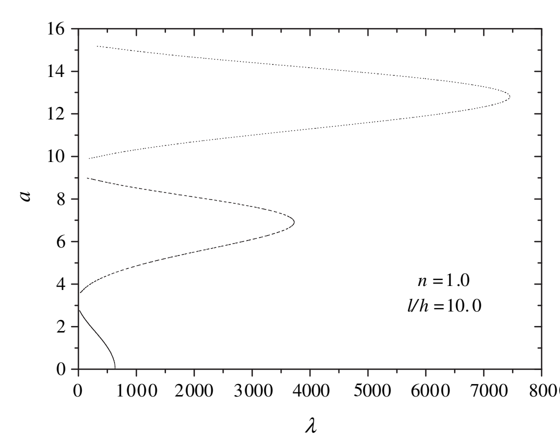

Fig. 5. Variation of parameter a with the thermal load, λ.

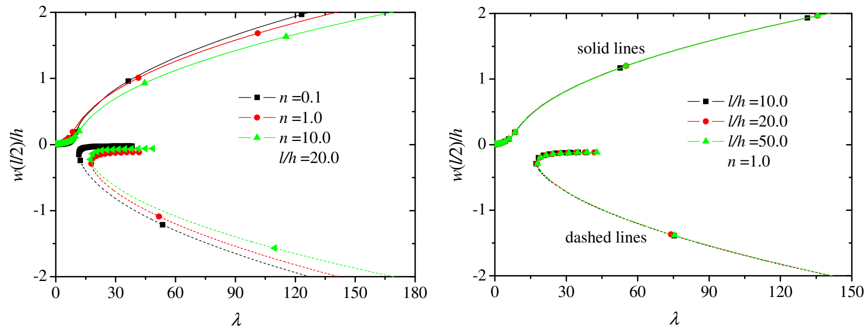

Fig. 6. Variation of the midspan deflection for a simply supported FGM beam with the thermal load, solid lines: $a \in (0, \pi)$, dashed lines: $a \in (\pi, 2\pi)$.

This can be rewritten as:

$$W^2 - \frac{16}{a_1^2}\Delta N = 0. \tag{39}$$

where $\Delta N = N - N_{cr}^F$. Since $N \geq N_{cr}^F$ or $\Delta N \geq 0$, only the post-buckling response of the FGM beam can be described by using Eq. (38) or Eq. (39). To describe the global responses including those of pre-buckling for the FGM beam, we can amalgamate Eq. (39) and a trivial solution, $W = 0$, into a single solution given by:

$$W\left(W^2 - \frac{16}{a_1^2}\Delta N\right) = 0. \tag{40}$$

Note that Eq. (40) is identical to the expressions given by Popov (2003) and Looss and Joseph (1990); these authors used the methods of bifurcation theory to obtain a simple algebraic equation that can describe the bifurcation buckling behavior of an Euler beam. When $\Delta N < 0$, i.e., $N < N_{cr}^F$, a real solution does not exist in either Eq. (38) or Eq. (39). Therefore, from Eq. (40), only a trivial solution, $W = 0$, is obtained, which represents the straight equilibrium configuration of an FGM beam. When$\Delta N > 0$, i.e., $N > N_{cr}^F$, both trivial and nontrivial solution branches simultaneously exist in Eq. (40), and the trivial solution is unstable, as pointed out by a number of researchers. The nontrivial solution in either Eq. (38) or Eq. (39) can accurately describe the post-buckling behavior of the beam, that is, the deflection of the FGM beam is nonlinear with the applied thermal load.

To understand the nonlinear static behavior of a metal/ceramic FGM beam subjected to an in-plane thermal loading, studies have been carried out on stainless steel (SUS304)-silicon nitride (Si_3N_4) FGM, which are the commonly used materials for FGMs in the existing studies. The material properties corresponding to Si_3N_4 and SUS304 are listed in Table 1. The result for the dimensionless critical thermal buckling load based on the exact solution obtained herein is compared with the corresponding result obtained by a shooting method (Ma and Lee, 2011) in Fig. 2. It can be observed from Fig. 2 that both of these agree extremely well with each other.

The typical thermal post-buckling paths of clamped FGM beams are shown in Fig. 3. Fig. 3a represents the results of these beams for various values of the gradient index, *n*, and Fig. 3b is for various values of the slenderness ratio, *l/h*. Also shown in Fig. 3a is the variation of the dimensionless midspan deflection with the dimensionless thermal loading, λ, for pure metal and ceramic beams. As expected, in Fig. 3a, it can be seen that the shape of the post-buckling load-deflection curves for FGM beams appears to be quite similar to that for pure material beams and the dimensionless midspan deflection of FGM beams with material properties between those of ceramic and metal is in between the deflections of the ceramic and metal beams. This can be attributed to the fact that the Young's modulus of ceramic is the highest and that of metal the lowest. It can be seen from Fig. 3b that the post-buckling deflection decreases with an increase in the slenderness ratio because this means a reduction in the influence of the transverse shear deformation. Fig. 4 gives the post-buckling configurations of clamped FGM beams.

3.2. Bending of a hinged–hinged FGM beam

For a hinged–hinged beam, the substitution of Eq. (28) into its boundary conditions, viz., Eq. (27), leads to:

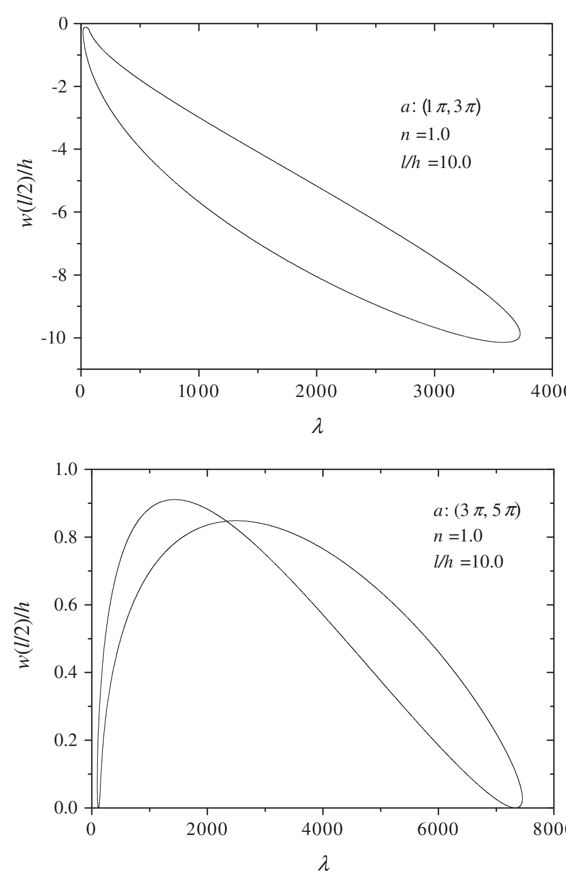

Fig. 7. Load-deflection curves of a simply supported FGM beam corresponding to parameter $a \in (\pi, 3\pi)$ and $a \in (3\pi, 5\pi)$.

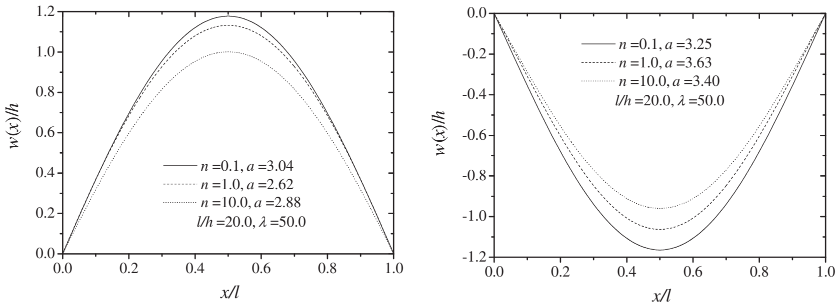

Fig. 8. Bending configurations of FGM beams simply supported at both ends.

$$W(0) = C_2 + C_4 = 0. \tag{41a}$$

$$W''(0) + F_2 M = -C_2 a^2 + \left(1 + F_1 a^2\right) M = 0. \tag{41b}$$

$$W(1) = C_1 \sin a + C_2 \cos a + C_3 + C_4 = 0. \tag{41c}$$

$$W''(1) + M = -C_1 a^2 \sin a - C_2 a^2 \cos a + \left(1 + F_1 a^2\right) M = 0. \tag{41d}$$

These conditions yield:

$$C_1 = c\tan\frac{a}{2}, \quad C_2 = c, \quad C_3 = 0, \quad C_4 = -c, \quad c = \left(1 + F_1 a^2\right) \frac{M}{a^2}. \tag{42}$$

Thus, the exact solution of the bended configuration for a beam with hinged–hinged boundary conditions can be expressed as:

$$W(X) = c\left\{\tan\frac{a}{2}\sin(aX) + \cos(aX) - 1\right\}. \tag{43}$$

Substituting Eq. (43) into Eq. (25) and using Eq. (24), one obtains:

$$c = \pm\sqrt{\frac{2}{\beta(1 + F_1 a^2) f(a)}}\sqrt{\frac{N}{a^2}\left(1 + F_1 a^2\right) - 1}. \tag{44}$$

where $f(a) = 1/1 + \cos a(1 - \sin a/a)$. Note that the parameter, a, in Eq. (43) is not a constant and varies with the applied thermal load N and M, as will be shown shortly.

The substitution of Eq. (43) into $\int_0^1 (\mathrm{d}W/\mathrm{d}X)^2 \mathrm{d}X$ leads to:

$$\int_0^1 \left(\frac{\mathrm{d}W}{\mathrm{d}X}\right)^2 \mathrm{d}X = c^2 a^2 f(a). \tag{45}$$

Substituting Eq. (45) into Eq. (25) and using Eq. (24) and the expression $c = (1 + F_1 a^2)\frac{M}{a^2}$, one obtains:

$$a^5(1 + \cos a) + \frac{\beta}{2} M^2 (a - \sin a)\left(1 + F_1 a^2\right)^3 - N a^3 \times \left(1 + F_1 a^2\right)(1 + \cos a) = 0. \tag{46}$$

where $a \neq 0, \ (2m - 1)\pi \quad m = 1, 2, \cdots$. Fig. 5 shows the variation of a with the dimensionless thermal load, λ. It is seen that depending on the load level, a may take on multiple values for a given load.

When $n = 0$, the thermal bending moment $M^{\mathrm{T}} = 0$. The boundary conditions for a hinged–hinged beam are homogeneous:

$$W = 0 \quad \text{and} \quad \frac{\mathrm{d}^2 W}{\mathrm{d}X^2} = 0 \quad \text{for a hinged end} \cdot \tag{47}$$

Thus, for a hinged–hinged homogeneous beam, Eq. (23) and the corresponding boundary conditions, viz., Eq. (47), lead to a differential eigenvalue problem. It can be easily proven that the solution for a hinged–hinged homogeneous beam is:

$$W(X) = c\sin(aX). \tag{48}$$

where $c = \pm 2\Big/\sqrt{1 + F_1 a^2}\sqrt{N/a^2 (1 + F_1 a^2) - 1}$. The characteristic equation for a corresponding to the simply supported boundary conditions is given by

$$\sin a = 0 \tag{49}$$

Based on FBT, Fig. 6 shows the variation of the dimensionless midspan deflection with the thermal load for a simply supported FGM beam. It is seen from Fig. 6 that simply supported FGM beams under an in-plane thermal load exhibit quite different behavior compared to the thermal post-buckling of clamped FGM beams, as shown in Fig. 3. Transverse displacements occur no matter how small the in-plane loads are; therefore, there is no bifurcation buckling for this case, which further confirms the conclusions made by several researchers in the existing literature (Leissa, 1986; Leissa, 1987; Qatu and Leissa, 1993; Shen, 2004). In Fig. 6, two different solution branches are seen to exist corresponding to two value intervals, $a \in (0, \ \pi)$ (solid lines) and $a \in (\pi, \ 2\pi)$ (dashed lines), respectively, which appear quite similar to the behavior corresponding to imperfect beams, as elaborated in Looss and Joseph (1990). Theoretically, the number of intervals that a may assume is infinite, i.e., $(0, \ \pi)$, $(\pi, \ 3\pi)$, $(3\pi, \ 5\pi)$, $\cdots$. As a result, the number of possible solution branches for the beams is infinite. Fig. 7 gives two solution branches for FGM beams corresponding to the intervals of a, $(\pi, \ 3\pi)$, $(3\pi, \ 5\pi)$, respectively; they are all closed. Note that Fig. 7 has no practical significance due to the extremely large value of the deflection or thermal load. Fig. 8 gives the bending configurations of simply supported FGM beams.

4. Conclusion

An exact, closed-form solution for the nonlinear static responses of FGM beams subjected to a uniform in-plane thermal loading is presented. The buckled configuration of beams with fixed–fixed boundary conditions and the bended configuration of beams with hinged–hinged boundary conditions were obtained as a function of the applied axial load. The exact solutions explicitly describe the nonlinear equilibrium paths of the deformed beam and thus are able to provide insights into deformation problems. The exact solutions obtained herein can serve as benchmarks to verify and improve various approximate theories and numerical methods.

Based on the exact solution, a nonlinear static behavior analysis of FGM beams has been carried out. The effects of various factors such as material constants, the transverse shear deformation, in-plane loading, and boundary conditions on the nonlinear mechanical behavior of FGM beams has been investigated by using the exact solution obtained herein. The following conclusions are arrived at from the present study.

1. Under an in-plane thermal loading, FGM beams fixed at both ends exhibit typical thermal post-buckling behavior. Also, all the beams with intermediate properties experience correspondingly intermediate values of the midspan deflection. The transverse deflection of a simply supported FGM beam subjected to an in-plane thermal load is initiated, regardless of the magnitude of the loading. As a consequence, bifurcation buckling does not occur for FGM beams that are simply supported at both ends. The load-deflection curve for simply supported beams has many different branches corresponding to different value intervals of the parameter, a.
2. An increase in the gradient index, n, results in an increase in the dimensionless critical buckling temperature for an FGM beam fixed at both ends and a decrease in the deflection of the beam.
3. An increase in the slenderness ratio, l/h, results in a reduction in the influence of transverse shear deformation. As a consequence, the dimensionless critical buckling temperature of classical beams is higher than that of shear deformable beams. In contrast, the deflection of classical beams is lower than that of shear deformable beams.

Acknowledgments

This work was supported by the Korea Science & Engineering Foundation through the NRL Program (Grant No. R0A-2007-000-10157-0), the WCU (World Class University) Program through the National Research Foundation of Korea funded by the Ministry of Education, Science, and Technology (R32-20087) and the National Natural Science Foundation of China (11072100).

References

Aydogdu, M., 2008. Conditions for functionally graded plates to remain flat under in-plane loads by classical plate theory. Compos. Struct. 82, 155–157.

Bhangale, R.K., Ganesan, N., 2006. Thermoelastic vibration and buckling analysis of functionally graded sandwich beam with constrained viscoelastic core. J. Sound. Vib. 295, 294–316.

Birman, V., Byrd, L.W., 2007. Modeling and analysis of functionally graded materials and structures. Appl. Mech. Rev. 60, 195–216.

Chakraborty, A., Gopalakrishnan, S., Reddy, J.N., 2003. A new beam finite element for the analysis of functionally graded materials. Int. J. Mech. Sci. 45 (3), 519–539.

Emama, S.A., Nayfeh, A.H., 2009. Postbuckling and free vibrations of composite beams. Compos. Struct. 88, 636–642.

Kapuria, S., Bhattacharyya, M., Kumar, A.N., 2008. Bending and free vibration response of layered functionally graded beams: a theoretical model and its experimental validation. Compos. Struct. 82 (3), 390–402.

Leissa, A.W., 1986. Conditions for laminated plates to remain flat under inplane loading. Compos. Struct. 6 (4), 262–270.

Leissa, A.W., 1987. A review of laminated composite plate buckling. Appl. Mech. Rev. 40 (5), 575–591.

Li, X.F., 2008. A unified approach for analyzing static and dynamic behaviors of functionally graded Timoshenko and Euler–Bernoulli beams. J. Sound. Vib. 318 (4–5), 1210–1229.

Librescu, L., Oh, S.Y., Song, O., 2005. Thin-walled beams made of functionally graded materials and operating in a high temperature environment: vibration and stability. J. Therm. Stresses 28, 649–712.

Looss, G., Joseph, D.D., 1990. Elementary Stability and Bifurcation Theory, second ed. Springer, New York.

Ma, L.S., Lee, D.W., 2011. A further discussion of nonlinear mechanical behavior for FGM beams under in-plane thermal loading. Compos. Struct. 93, 831–842.

Ma, L.S., Ou, Z.Y., Huang, D.W., 2006. Analytical relationships of simply-supported beam's eigenvalues using different beam theories. Eng. Mechanics 23 (10), 91–95 (in Chinese).

Ma, L.S., Wang, T.J., 2003a. Nonlinear bending and post-buckling of a functionally graded circular plate under mechanical and thermal loadings. Int. J. Solids Struct. 40 (13–14), 3311–3330.

Ma, L.S., Wang, T.J., 2003b. Axisymmetric post-buckling of a functionally graded circular plate subjected to uniformly distributed radial compression. Mater. Sci. Forum 423–424, 719–724.

Morimoto, T., Tanigawa, Y., Kawamura, R., 2006. Thermal buckling of functionally graded rectangular plates subjected to partial heating. Int. J. Mech. Sci. 48, 926–937.

Popov, A.A., 2003. Parametric resonance in cylindrical shells: a case study in the nonlinear vibration of structural shells. Eng. Struct. 25, 789–799.

Qatu, M.S., Leissa, A.W., 1993. Buckling or transverse deflections of unsymmetrically laminated plates subjected to in-plane loads. AIAA J. 31 (1), 189–194.

Shen, H.S., 2002. Nonlinear bending response of functionally graded plates subjected to transverse loads and in thermal environments. Int. J. Mech. Sci. 44, 561–584.

Shen, H.S., 2004. Bending, buckling and vibration of functionally graded plates and shells. Adv. Mechanics 34 (1), 53–60 (in Chinese).

Yang, J., Chen, Y., 2008. Free vibration and buckling analyses of functionally graded beams with edge cracks. Compos. Struct. 83 (1), 48–60.

Ying, J., Lu, C.F., Chen, W.Q., 2008. Two-dimensional elasticity solutions for functionally graded beams resting on elastic foundations. Compos. Struct. 84, 209–219.

Zhang, D.G., Zhou, Y.H., 2008. A theoretical analysis of FGM thin plates based on physical neutral surface. Comput. Mater. Sci. 44, 716–720.

Zhong, Z., Yu, T., 2007. Analytical solution of a cantilever functionally graded beam. Compos. Sci. Technol. 67, 481–488.